Journal of Biological Methods | **2020** | **Vol**. 7(3) | e136
DOI: 10.14440/jbm.2020.335

**PROTOCOL**

# A simple and robust cell-based assay for the discovery of novel cytokinesis inhibitors

Laszlo Radnai[1,2], Rebecca F. Stremel[1,2], Thomas Vaissiere[2], Li Lin[1], Michael Cameron[1], William H. Martin[3], Gavin Rumbaugh[2], Theodore M. Kamenecka[1], Patrick R. Griffin[1], Courtney A. Miller[1,2]*

[1]Department of Molecular Medicine, The Scripps Research Institute, Jupiter, FL 33458, USA
[2]Department of Neuroscience, The Scripps Research Institute, Jupiter, FL 33458, USA
[3]WHM Consulting, LLC, 111 Sterling City Rd., Lyme, CT 06371, USA

*Corresponding author: Courtney A. Miller, Email: cmiller@scripps.edu

Competing interests: The authors have declared that no competing interests exist.

Abbreviations used: DMSO, dimethyl sulfoxide; NCR, nuclei-to-cell ratio; NMII, nonmuscle myosin II; PI, propidium iodide

Received April 22, 2020; Revision received May 31, 2020; Accepted June 28, 2020; Published September 17, 2020

## ABSTRACT

Cytokinesis is the last step of mitotic cell division that separates the cytoplasm of dividing cells. Small molecule inhibitors targeting either the elements of the regulatory pathways controlling cytokinesis, or the terminal effectors have been of interest as potential drug candidates for the treatment of various diseases. Here we present a detailed protocol for a cell-based cytokinesis assay that can be used for the discovery of novel cytokinesis inhibitors. The assay is performed in a 96-well plate format in 48 h. Living cells, nuclei and nuclei of dead cells are identified by a single staining step using three fluorescent dyes, followed by rapid live cell imaging. The primary signal is the nuclei-to-cell ratio (NCR). In the presence of cytokinesis inhibitors, this ratio increases over time, as the ratio of multinucleated cells increases in the population. The ratio of dead nuclei to total nuclei provides a simultaneous measure of cytotoxicity. A screening window coefficient (*Z*`) of 0.65 indicates that the assay is suitable for screening purposes, as the positive and negative controls are well-separated. $EC_{50}$ values can be reliably determined in a single 96-well plate by using only six different compound concentrations, enabling the testing of 4 compounds per plate. An excellent test-retest reliability ($R^2$ = 0.998) was found for $EC_{50}$ values covering a ~1500-fold range of potencies. Established small molecule inhibitors of cytokinesis operating *via* direct action on actin dynamics or nonmuscle myosin II are used to demonstrate the robustness, simplicity and flexibility of the assay.

**Keywords:** drug discovery, actin cytoskeleton, screening, multinucleated, cytotoxicity

## BACKGROUND

In all eukaryotic cells, mitosis is the complex cytological process that separates the already duplicated chromosomes in space into two identical sets, ultimately leading to the formation of two fully functional nuclei in distant parts of the cell [1]. Mitosis is followed by cytokinesis, a process that separates the cytoplasm of dividing cells resulting in the formation of two daughter cells [2,3]. In animals, a contractile ring of filamentous actin and nonmuscle myosin II (NMII) assembles in the equatorial plane of the dividing cells (between the segregated sister chromatids) that splits the cytoplasm during cytokinesis by forming the so-called cleavage furrow. The process is tightly regulated both in space and time [2-5].

Cytokinesis inhibitors targeting actin, NMII or other regulatory and structural elements necessary for the proper functioning of the cleavage furrow have not only provided useful information about the function of these elements, but are increasingly recognized as potential drug candidates [6]. For example, NMII has been reported as a potential therapeutic target for the prevention of relapse to methamphetamine use [7,8]. Targeting NMII by using the small molecule inhibitor blebbistatin resulted in the selective disruption of methamphetamine-associated memories in animal model systems [7,8]. Blebbistatin also showed antitumorigenic properties in human hepatocellular carcinoma cells by reducing the NMII-mediated intracellular trafficking of the RNA-binding protein HuR, thereby reducing pathologic posttranscriptional gene expression [9]. Targeting the serine/threonine kinase Aurora B with small molecule inhibitors has been shown to block cytokinesis and induce a multinucleated phenotype in cell cultures [10,11]. The overexpression of Aurora B correlates with poor prognosis in several human cancer types [12]. Inhibition of Aurora B activity has been found to inhibit

**How to cite this article:** Radnai L, Stremel RF, Vaissiere T, Lin L, Cameron M, Martin WH, Rumbaugh G, Kamenecka TM, Griffin PR, Miller CA. A simple and robust cell-based assay for the discovery of novel cytokinesis inhibitors. *J Biol Methods* 2020;7(3):e136. DOI: 10.14440/jbm.2020.335

proliferation and induce tumor regression in animal model systems. Several small molecule inhibitors of Aurora B are currently under phase I/II evaluation or preclinical testing [12].

Here we present a cell-based assay that is amenable to the discovery of novel cytokinesis inhibitors. The assay is run in 96-well plates with a total incubation time of 48 h. We demonstrate the robustness, flexibility and reliability of the assay by using small molecule inhibitors of NMII (blebbistatin, *para*-aminoblebbistatin and *para*-nitroblebbistatin) and modulators of actin dynamics with different mechanisms of action (jasplakinolide, cytochalasin D and swinholide A). Blebbistatin blocks cellular blebbing and disrupts directed cell migration [13]. It also blocks cytokinesis by inhibiting the contraction of the cleavage furrow [13]. *Para*-nitroblebbistatin and *para*-aminoblebbistatin are photostable derivatives of blebbistatin with reduced cytotoxicity [14,15]. *Para*-aminoblebbistatin also shows substantially improved water solubility [15]. Jasplakinolide is a stabilizer of pre-formed actin filaments and an inducer of actin polymerization *in vitro* [16,17]. By facilitating filament nucleation and lowering the critical actin concentration, jasplakinolide treatment results in the formation of amorphous actin masses in cultured cells [17]. Cytochalasin D inhibits actin polymerization *in vitro* by binding to the net polymerizing ends of actin filaments and blocking the addition of new monomers to these sites [18,19]. It also binds actin monomers, inducing the formation of dimers and thereby increasing the rate, but decreasing the extent of polymerization [20,21]. In cells, cytochalasin D treatment leads to the disruption of the cytoskeletal actin filament network and the aggregation of actin filaments [22,23]. The third modulator of actin polymerization used here, Swinholide A, is a highly potent toxin that rapidly severs actin filaments *in vitro* [24], and disrupts the actin cytoskeleton of living cells *in vivo* [24,25]. All of these compounds were used to test our assay, as it is well-established that they induce the accumulation of binucleated cells in culture [13-15,24,26,27].

## MATERIALS

### Reagents, media and solutions

- ✓ Cultured cells (COS-7 are used here as example. However, any cell that undergoes cytokinesis in culture is expected to be amenable to this protocol. COS-7 Cat. # CRL-1651, American Type Culture Collection, Manassas, VA)
- ✓ Dulbecco's Modified Eagle Medium (Cat. # 11995073, Life Technologies, Carlsbad, CA)
- ✓ Fetal Bovine Serum (Cat. # 26140079, Life Technologies, Carlsbad, CA)
- ✓ Antibiotic-Antimycotic solution (Cat. # 15240062, Life Technologies Carlsbad, CA)
- ✓ 75 $cm^2$ flasks (Cat. # 430641U, Corning, Corning, NY)
- ✓ Dulbecco's phosphate-buffered saline (PBS, Cat. # 14190250, Life Technologies, Carlsbad, CA)
- ✓ Trypsin-EDTA (0.25%) solution (Cat. # 25200072, Life Technologies, Carlsbad, CA)
- ✓ 96-well cell culture plates (Cat. # 25109, Genesee Scientific, El Cajon, CA)
- ✓ Jasplakinolide (Cat. # 2792/100U, R&D Systems (Minneapolis, MN)
- ✓ Cytochalasin D (Cat. # 113305, Cayman Chemical, Ann Arbor, MI)
- ✓ Swinholide A (Cat. # 501146229, Fisher Scientific, Hanover Park, IL)
- ✓ Blebbistatin (Cat. # 13013, Cayman Chemical, Ann Arbor, MI)
- ✓ *para*-aminoblebbistatin (Cat. # 22699, Cayman Chemical, Ann Arbor, MI)
- ✓ *para*-nitroblebbistatin (Cat. # 24171, Cayman Chemical, Ann Arbor, MI)
- ✓ Dimethyl sulfoxide (DMSO, Cat. # D2650, Sigma-Aldrich, St. Louis, MO)
- ✓ Solvent resistant polypropylene microplates (Cat. # 3357, Corning, Corning, NY)
- ✓ Fluorescein diacetate (FDA, Cat. # F7378, Sigma-Aldrich, St. Louis, MO)
- ✓ Hoechst33342 (Cat. # H3570, Life Technologies, Carlsbad, CA)
- ✓ Propidium iodide (PI, Cat. # P3566, Life Technologies, Carlsbad, CA)

### Recipes

- ✓ Culture medium: 89% Dulbecco's Modified Eagle Medium, 10% Fetal Bovine Serum, and 1% Antibiotic-Antimycotic solution.

### Equipment

- ✓ Refrigerated centrifuge (Cat. # 5430 R, Eppendorf, Hauppauge, NY)
- ✓ Microplate shaker (Cat. # 12620-926, VWR, West Chester, PA)
- ✓ Fluorescence microscope (*e.g.*, IN Cell Analyzer 6000 automated fluorescence microscope, Cat. # 29043323, GE Healthcare BioSciences, Marlborough, MA)
- ✓ Image analysis software (*e.g.*, IN Cell Developer Toolbox software, Cat. # 25809826, GE Healthcare Bio-Sciences, Marlborough, MA)

## PROCEDURE

### Culturing cells

A simplified protocol flowchart is shown in **Figure 1**.

1. Thaw frozen aliquots of cell line of interest and immediately dilute ten-fold in culture medium.
2. Centrifuge the cell suspension at 7197 × *g* at 20°C for 10 min in a refrigerated centrifuge.
3. Discard the supernatant and resuspend the pellet in culture medium at a final density of ~50000 cells/ml.

4. Plate cells onto 75 $cm^2$ flasks at a density of 500000 cells/flask.
5. Following 3 d of incubation (37°C and 5% $CO_2$), remove old media from the flasks and wash the cell layers twice with 5 ml of PBS.
6. Add 2 ml of Trypsin-EDTA (0.25%) solution to each flask to dissociate cells.
7. Incubate flasks at 37°C for 10 min to allow detachment of cells from the surface.
8. Cell dissociation can be further facilitated by pipetting the suspension up and down several times until no cell aggregates are observed by visual inspection under a stereomicroscope.
9. To inhibit trypsin, combine 8 ml of fresh culture medium with 2 ml of cell suspension.
10. Determine cell density by counting the cells in a hemocytometer.
11. Dilute the suspension to a density of 20000 cells/ml.
12. Immediately plate cells onto flat bottom, 96-well cell culture plates by transferring 100 µl of suspension to each well using a multichannel pipette, resulting in a final surface density of 2000 cells/well.

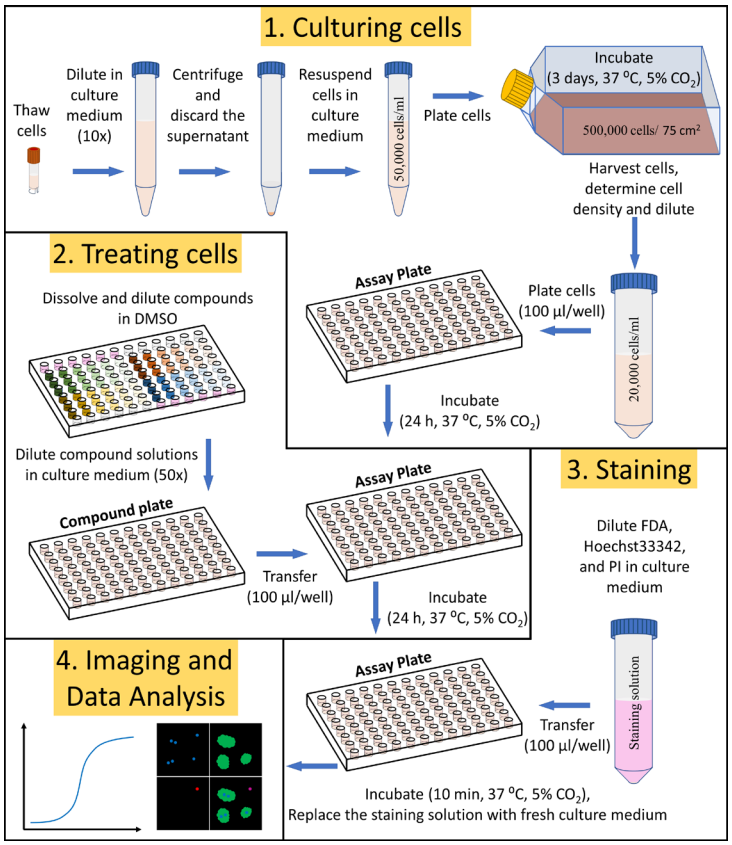


**Figure 1. Protocol flowchart.**

## Treating cells

13. Following 24 h of incubation (37°C, 5% $CO_2$), treat cells with compounds of interest prepared in compound plates.
14. Here, jasplakinolide, cytochalasin D, swinholide A, blebbistatin, *para*-aminoblebbistatin or *para*-nitroblebbistatin were first dissolved in DMSO.
15. Six-step serial 1:2 dilutions of compound solutions were then prepared in DMSO using solvent resistant polypropylene microplates. Concentration ranges (125–3.91 nM, 500–15.63 nM, 10–0.31 nM, 10–0.31 µM, 10–0.31 µM, and 10–0.31 µM for jasplakinolide, cytochalasin D, swinholide A, blebbistatin, *para*-aminoblebbistatin and *para*-nitroblebbistatin, respectively) were determined based on preliminary results. A 2 mM solution of *para*-aminoblebbistatin in DMSO was also prepared and used as positive control, while pure DMSO was used as a negative control.

16. Prepare compound plates by transferring 2.4 µl of positive and negative controls and compound solutions into each well of a 96-well plate containing 117.6 µl of culture media (50-fold dilution) using a multichannel pipette. Wells in the first and last rows should be used exclusively for negative and positive controls.

17. Mix solutions by shaking the compound plate for 1 min at room temperature at 1200 rpm using a microplate shaker. A typical plate layout map used for screening experiments is shown in **Figure S1**. Carry out all measurements in triplicate.

18. Transfer 100 µl of diluted compound solutions from the compound plate to the assay plate (containing cell cultures in 100 µl of culture media) using a multichannel pipette (2-fold dilution).

**TIP:** The DMSO concentration in the compound and assay plate is 2% and 1%, respectively. The final concentration of the positive control *para*-aminoblebbistatin is 20 µM, resulting in ~100% signal. (see **Fig. 2** and **3** and Anticipated results and troubleshooting section for more details.) All steps using blebbistatin or derivatives are performed under limited light conditions to minimize photochemical inactivation of compounds or potential phototoxic effects [28].

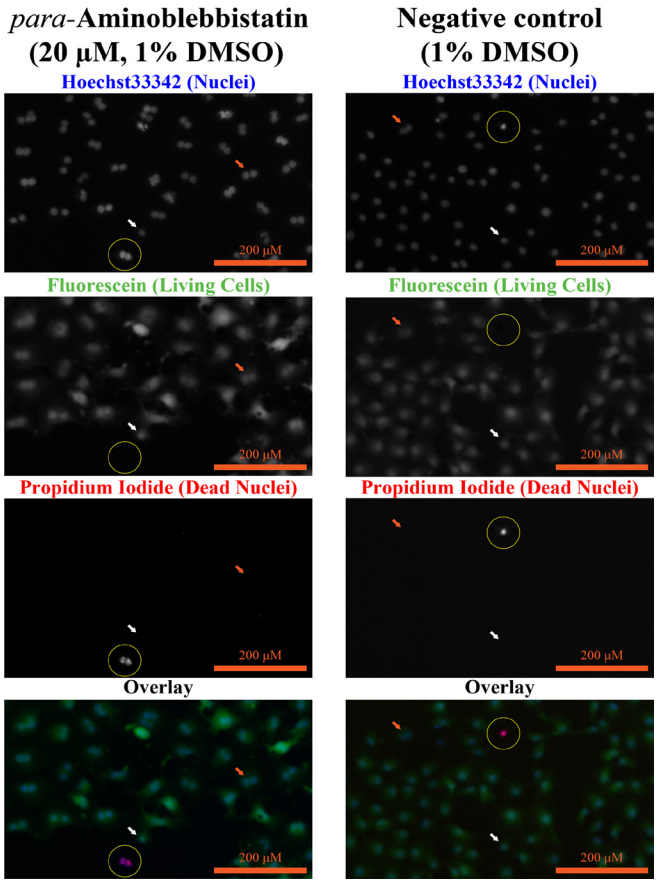


**Figure 2. Representative images of *para*-aminoblebbistatin treated and control cells.** Cells were incubated for 24 h in the presence of 20 µM *para*-aminoblebbistatin (left) or 1% DMSO as a negative control (right). Nuclei, living cells and nuclei of dead cells were visualized by Hoechst33342, FDA and PI staining, respectively. Overlaid images are shown to guide the eyes (lower panels, nuclei—blue, living cells—green, dead nuclei—red). Most of the *para*-aminoblebbistatin treated cells are bi- or multinucleated and much bigger than negative control cells, which are primarily mononucleated. Examples of a mono- (white arrows) and a binucleated cell (orange arrows) are highlighted in each image. Note that there is no living cell body revealed around the nuclei showing PI staining (yellow circles). However, these nuclei are positive for both Hoechst33342 and PI, confirming their identity. Images were not manipulated other than changing the brightness and contrast for visibility. No changes were made to images prior to analysis.

## Staining cells

The presence of cytokinesis inhibitors in cell culture leads to the accumulation of multinucleated cells. For example, treating COS-7 cells with 20 µM *para*-aminoblebbistatin for 24 h results in a cell population where most cells are binucleated (**Fig. 2**). FDA, a membrane-permeant non-fluorescent cell viability dye that is hydrolyzed to fluorescein in living cells [29] by naturally present esterase enzymes [30] can be used to visualize the cytoplasm. The resulting prod-

uct, fluorescein, accumulates in the cytoplasm, giving a bright green fluorescence signal [29]. The result is an excellent signal-to-noise ratio. Nuclei can be visualized by Hoechst33342, a cell-permeable DNA stain [31]. The excitation and emission peaks of Hoechst33342 (ex: 350 nm, em: 461 nm, DNA-bound) and fluorescein (ex: 490 nm, em: 526 nm) are well-separated from each other. Therefore, these dyes can be used in parallel in imaging applications. However, as the areas highlighted in **Figure 2** demonstrate, not all nuclei revealed by Hoechst33342 staining overlap with living cells. A second DNA dye, propidium iodide (PI) [32], which is membrane-impermeant [33] can be used to confirm the identity of these objects. This dye is widely used to stain nuclei of dead cells in a cell population [34]. The spectral properties of PI (ex: 535 nm, em: 617 nm, DNA-bound) enable its use in parallel with the other two dyes, to identify compounds' potential cytotoxicity.

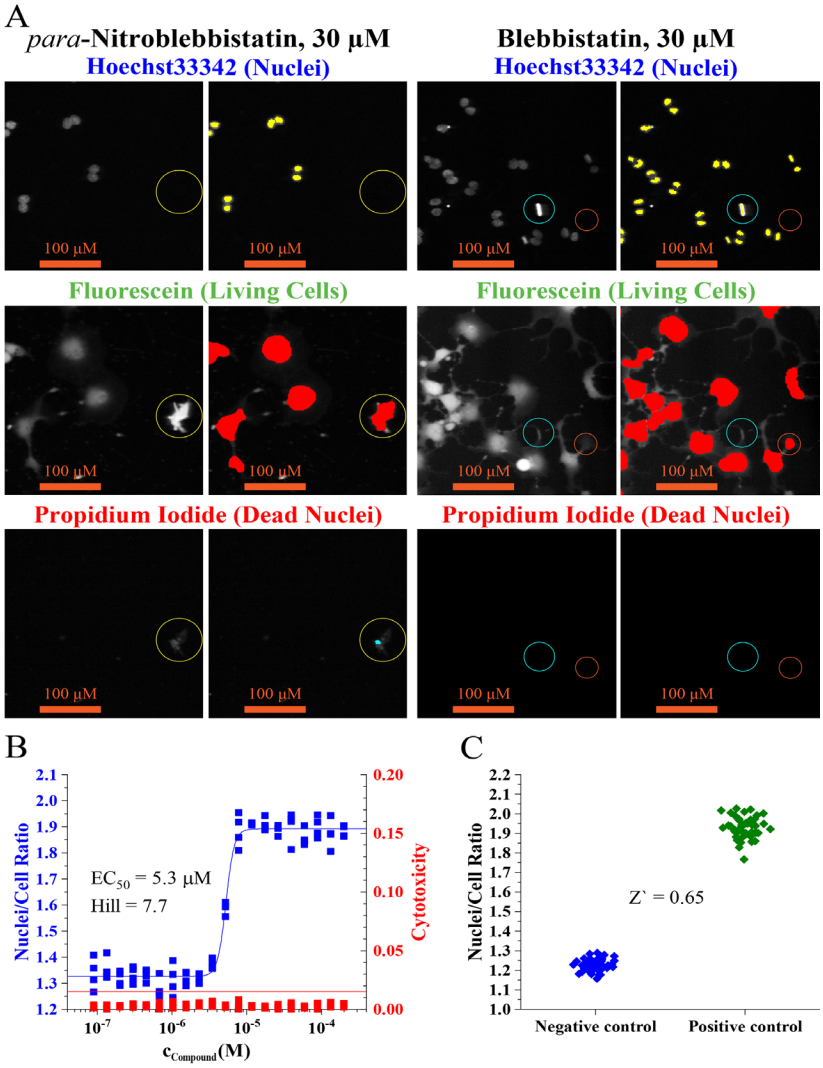


**Figure 3. Image analysis and control selection. A.** Potential artifacts may result from compound precipitation and object misidentification during image analysis. COS-7 cells were treated with *para*-nitroblebbistatin and blebbistatin at 30 µM. Left and right panels show raw images and detected objects (nuclei—yellow, living cell—red, dead nuclei—cyan), respectively, for both compounds. Crystals of *para*-nitroblebbistatin (yellow circles) showed green and red fluorescence, while blebbistatin crystals (cyan circles) showed blue fluorescence. Accordingly, the *para*-nitroblebbistatin crystal cluster shown was initially misidentified as a living cell and also as a dead nucleus, while the blebbistatin crystal was misidentified as an elongated nucleus. Based on cell shape and size, parts of the cytoplasm can also be misidentified as separate cells (orange circles). However, since those "cells" not overlapping with nuclei, those "nuclei" not overlapping with cells or those "dead nuclei" not showing labeling for both Hoechst33342 and PI are excluded from our calculations, these artifacts usually have only limited effect on our signals. **B.** *Para*-aminoblebbistatin was selected as a positive control due to its high solubility, photostability and low cytotoxicity [15]. By fitting the dose response data to the Hill equation, an $EC_{50}$ of 5.3 µM with a very steep transition (Hill constant = 7.7) was determined. The signal approaches its maximum value around and above ~10 µM compound concentration, therefore, 20 µM *para*-aminoblebbistatin was chosen as a reliable positive control in this work. (The red horizontal line represents the cytotoxicity threshold of 0.015. See text for further explanation.) **C.** A *Z`* [35] of 0.65 was determined for a half plate of negative (1% DMSO) and half plate of positive controls (1% DMSO, 20 µM *para*-aminoblebbistatin), indicating a reliable assay for screening with well-separated positive and negative controls.

19. Following 24 h of incubation in the presence of compounds (37°C, 5% $CO_2$), stain cells with FDA, Hoechst33342 and PI in a single step.

20. Prepare staining solution by combining 9 µl FDA (24 mM stock solution in DMSO), 22.2 µl Hoechst33342 (16.2 mM stock solution in water), 96 µl PI (1.5 mM stock solution in water) and 11.873 ml culture medium in a 50 ml centrifuge tube for each plate.

21. Use a multichannel pipette to add 100 µl of staining solution to each well of the assay plate containing 200 µl of treated cell culture, resulting in a final concentration of 6 µM, 10 µM, and 4 µM for FDA, Hoechst33342 and PI, respectively.

22. Incubate assay plates for 10 min (37°C, 5% $CO_2$).

23. Replace the staining solution with fresh culture medium in each well (100 µl/well).

**TIP:** Due to the photosensitivity of some of the compounds used and to limit photochemical degradation of the fluorescent dyes, the incubation steps were performed in darkness and all other steps were performed under limited light conditions.

## Imaging

A fluorescence microscope is needed for imaging. Here, an IN Cell Analyzer 6000 automated fluorescence microscope and accompanying software was used. Image acquisition was performed using the Nikon 10×/0.45, Plan Apo, CFI/60 objective.

24. Lasers operating at 405 nm, 488 nm, and 561 nm in conjunction with 455 nm, 525 nm and 605 nm emission filters are used for the visualization of Hoechst33342, fluorescein and PI signals, respectively.

**TIPS:** Cultures do not need to be incubated during imaging because both cells and nuclei remain detectable without a change in morphology or number for hours at room temperature. Count cells while imaging to ensure that at least 600 cells per well are imaged. Lower cell counts may yield unreliable results. (See Discussion section for a detailed statistical explanation.)

## Data analysis

25. Identify and quantify nuclei of living and dead cells by using the corresponding fluorescent signal of Hoechst33342. Cell bodies of living cells are identified by using the corresponding fluorescent signal of fluorescein. Nuclei of dead cells are identified by using the corresponding fluorescent signal of PI.

26. If using the IN Cell Developer Toolbox software, nuclear segmentation (Hoechst33342) can be performed using the following parameters: minimum target area: 85 µm$^2$, sensitivity: 50, sensitivity range 1.30, precise mask: enabled. Steps of postprocessing: watershed clump breaking, erosion (kernel size 9), sieve (keep targets with an area greater than 20 µm$^2$), border object removal. Cytoplasm segmentation (fluorescein) can be performed using the following parameters: noise suppression: heavy, remove shading artifacts with area greater than: 2960 µm$^2$, use octagonal morphology: enabled. Steps of postprocessing: sieve (keep targets with an area greater than 200 µm$^2$), erosion (kernel size 3), watershed clump breaking, fill holes, dilation (kernel size 3), sieve (keep targets with an area greater than 200 µm$^2$), border object removal. Nuclear segmentation (PI) can be performed using the following parameters: minimum target area 52 µm$^2$, sensitivity: 20, sensitivity range 1.30, precise mask-enabled, use octagonal morphology: enabled. Steps of postprocessing: watershed clump breaking, erosion (kernel size 5), sieve (keep targets with an area greater than 20 µm$^2$), border object removal.

**TIP:** This analysis is possible with any software tool capable of segmenting and counting cells and nuclei. The specific segmentation and analysis protocol file used for the IN Cell Developer Toolbox is available to researchers upon request.

27. A cytokinesis inhibitor allows nuclei to divide, but blocks the separation of cell bodies, resulting in the formation of bi- and multinucleated cells. The inhibitory effect of compounds can be estimated and compared by calculating the ratio of nuclei to cell numbers in the living cell population. Each living cell must contain at least one nucleus and each nucleus must belong to a living cell in this population. Therefore, fluorescein-positive objects not overlapping with Hoechst33342-positive objects (potentially misidentified cells) and Hoechst33342-positive objects not overlapping with fluorescein-positive (dead and potentially misidentified

nuclei) should be excluded from the calculation of the nuclei-to-cell ratio (NCR). This step was crucial to avoid several artifacts (see Anticipated results and troubleshooting and Discussion).

***28.*** In addition to cytokinesis inhibition, compounds may show cytotoxic effects, which can affect the primary signal (*e.g.*, through nuclear fragmentation or selective death of multinucleated cells). Therefore, cytotoxicity should also be quantified as the ratio of dead nuclei to total nuclei. Dead nuclei must show positive staining for both Hoechst33342 and PI. Therefore, all those objects not showing double labeling should be excluded from this calculation. Similarly, the total number of nuclei are calculated as the sum of Hoechst33342-positive objects overlapping with fluorescein-positive objects (living nuclei) and the Hoechst33342-positive objects overlapping with PI-positive objects (dead nuclei).

***29.*** Plot the NCR against the compound concentration. To determine the half maximal effective concentration ($EC_{50}$), fit the 6 point dose response data to the Hill equation:

$$\textbf{Eqn. 1}\ ,\ NCR = NCR_{min} + \left(NCR_{max} - NCR_{min}\right)\left(1 - \frac{1}{1 + \left(\frac{c_{inh}}{EC_{50}}\right)^{Hill}}\right)$$

where $c_{inh}$ is the concentration of the compound, $NCR_{min}$ is the NCR in the absence of inhibitors, $NCR_{max}$ is the extrapolated value of the NCR at 100% inhibition, and *Hill* is the Hill-constant.

**TIP:** The NCR is always expected to be greater than 1 in all actively dividing cell cultures, including controls, because there is always a subpopulation of dividing cells that will contain two nuclei.

## Anticipated results and troubleshooting

To quantify the inhibitory effect of the actin and myosin compounds, we quantified Hoechst33342, fluorescein, and PI-positive objects, representing nuclei, living cells, and dead nuclei, respectively. Then, we calculated the NCR for each sample (cells from the same well) by dividing the number of nuclei that overlap with living cells (living nuclei) with the number of those living cells overlapping with nuclei. (Every cell must contain at least one nucleus and every nucleus belongs to a cell.) Cytotoxicity was also quantified as the ratio of dead nuclei to all nuclei. Here, only the double-labeled (Hoechst33342 and PI-positive) nuclei were counted as dead nuclei. The total number of nuclei was calculated as the sum of the double-labeled dead nuclei and the above defined living nuclei. With this strategy, several artifacts resulting from object misidentification could be efficiently avoided.

One main source of artifacts is the limited solubility of the compounds in culture media. Solubility in culture media is often not known for novel compounds and aqueous solubility; if known, may not reflect a compound's solubility in culture media at 37°C. Applying compounds at concentrations higher than their solubility limit may result in compound precipitation. This is notable because precipitates may show fluorescence in one or more channel and may be similar in shape and size to cells or nuclei. As a result, compound precipitates are prone to misidentification as target objects (cells or nuclei). To demonstrate the effect of compound precipitation, we treated COS-7 cells with *para*-nitroblebbistatin and blebbistatin at 30 µM. The kinetic aqueous solubility of blebbistatin and *para*-nitroblebbistatin has been reported to be 9.3 µM and 3.6 µM, respectively [15]. Since 30 µM was much higher than the solubility in both cases, the compounds precipitated as expected, and fluorescent crystals attached to the surface were detected (**Fig. 3A**). Crystals of *para*-nitroblebbistatin showed bright green fluorescence and a detectable signal in the red channel. Blebbistatin crystals showed bright blue fluorescence. Accordingly, *para*-nitroblebbistatin crystals were prone to be misidentified as living cells and also as dead nuclei. Blebbistatin crystals were prone to be misidentified as nuclei. However, our method of using double fluorescent labeling for every object of interest (living cells must overlap with nuclei; nuclei must overlap with either living cells or dead nuclei; dead nuclei must overlap with nuclei) resulted in our analysis being resistant to these artifacts. This strategy also helped to avoid misidentification of any parts of the cytoplasm as a separate cell (**Fig. 3A**) or misidentification of potential fluorescent contamination present in the field of view.

Even for cell populations where no precipitation-related artifacts were present, the number of misidentified objects was effectively reduced by applying the rules detailed above. For example, ~90000 and ~110000 Hoechst33342-positive objects, ~68000 and ~62000 fluorescein-positive objects, and ~1000 and ~1300 PI-positive objects were identified for 96 wells of negative (1% DMSO) and positive controls (1% DMSO, 20 µM *para*-aminoblebbistatin; see below) across 8 plates, respectively. To calculate NCR, only ~94% and ~93% of Hoechst33342-positive objects ("nuclei", overlapping with fluorescein-positive objects) and 97% and 88% of fluorescein-positive objects ("living cells", overlapping with Hoechst33342-positive objects) were used, respectively. To calculate cytotoxicity, only ~60% and 57% of PI-positive objects ("dead nuclei", PI and Hoechst33342 double-positive), and ~95% and ~94% of Hoechst33342-positive objects ("total number of nuclei", Hoechst33342-positive objects overlapping either with fluorescein- or PI-positive objects) were used, respectively. The rejected objects were either misidentified fluorescent objects, or correctly identified parts of cell bodies or nuclei along the edges of the image where the overlapping nuclei or cell bodies had been rejected during image analysis. (It is not possible to accurately quantify the number of nuclei if the whole cell is not visible.)

Precipitation may not only lead to fluorescent artifacts, but also limit the effective concentration of the compound, resulting in limited signal

in single-point or dose-response experiments. Moreover, precipitates are usually not tolerated well by living cells. Elevated cytotoxicity may be a good indicator of this problem. The intrinsic toxicity of the compound might also result in higher levels of observed cytotoxicity. Significant levels of cytotoxicity can only be determined empirically. Negative and positive controls across 8 plates (96 wells each) showed an average cytotoxicity of 0.007 ± 0.009 and 0.007 ± 0.005, respectively. More than 90% of the data points were under the level of 0.015 in both categories. Therefore, a cytotoxicity signal equal to or greater than ~0.015, corresponding to ~1.5% dead nuclei in the population, was considered significant. Around and above this threshold, deterioration of the NCR signal was usually observed, further supporting the idea that our threshold was set to the appropriate level. In addition to the limited effective concentration due to solubility issues, selective loss of multinucleated cells, cell clustering, cell detachment from the surface, abnormal morphology or nuclear fragmentation may cause deviation of the NCR signal from the expected value. Analyzing any signal where the associated cytotoxicity is too high should be generally avoided.

*Para*-aminoblebbistatin is known as a non-cytotoxic derivative of the myosin inhibitor blebbistatin, showing greatly improved photostability and solubility [15]. These properties make it an excellent positive control in the cytokinesis assay. The potency ($EC_{50}$) of *para*-aminoblebbistatin was determined in dose-response experiments (**Fig. 3B**). An $EC_{50}$ of 5.3 µM was found by fitting the NCR signal to the Hill equation (**Eqn. 1**). Previously, *para*-aminoblebbistatin was shown to inhibit the proliferation of HeLa cells with a similar $EC_{50}$ value (~18 µM) [15]. Interestingly, the dose-response curve determined here showed a very steep transition (Hill constant = 7.7), such that the signal approached 100% around 10 µM compound concentration. To ensure that the inhibition level is always around 100%, we chose 20 µM as the positive control concentration for *para*-aminoblebbistatin. Consistent with the literature [15], no significant cytotoxicity was observed up to 200 µM concentration. The $Z`$ (also known as the screening window coefficient) is a widely used statistical parameter that helps to assess the reliability of screening data [35]. We determined the $Z`$ for a half plate of negative (1% DMSO) and a half plate of positive (1% DMSO, 20 µM *para*-aminoblebbistatin) controls:

$$\textbf{Eqn. 2}\ ,\ Z` = 1 - \frac{3\left(\sigma_p + \sigma_n\right)}{\left|\mu_p - \mu_n\right|}$$

where $\sigma_n$, $\sigma_p$ and $\mu_n$, $\mu_p$ are the sample standard deviations and means of the negative and positive controls, respectively (**Fig. 3C**). We found a $Z` > 0.5$ ($Z` = 0.65$), which indicates that the assay is excellent for screening purposes [35].

Next, we treated COS-7 cells with dilution series of blebbistatin, *para*-aminoblebbistatin, *para*-nitroblebbistatin, jasplakinolide, cytochalasin D or swinholide A. Although these compounds have different molecular targets and mechanisms of action, they all inhibit cytokinesis [13-15,24,26,27]. Accordingly, cells developed similar, bi- and multinucleated phenotypes in response to all compounds (**Fig. 4**, **Fig. S2** and **S3**). Although slightly different cellular morphology was observed, our robust strategy (simply counting cells and nuclei instead of attempting to classify individual cells based on their phenotype) was effective in the quantitation of the inhibitory activity in all cases.

Dose-response curves with very steep transitions (Hill constants between 5.2 and 7.7) were observed (**Fig. 5**). By using only six-step serial 1:2 dilutions and performing every experiment in triplicate, it was possible to obtain reliable $EC_{50}$ data for four compounds on a single 96-well plate (For $EC_{50}$ values, see **Fig. 5** and the upper right panel in **Fig. 6**. See **Fig. S1** for plate layout). Repeated experiments with fresh cell cultures yielded similar $EC_{50}$ values (**Fig. 6**). To quantitate the reliability of the assay, linear regression analysis was performed using the data from both runs. A coefficient of determination of 0.998 showed excellent test-retest reliability (**Fig. 6**).

Note that the "dense sampling" of the dose response curves (1:2 dilutions), together with the observed steep transitions constrain the possible values of the $EC_{50}$ in a less than two-fold range, even if other parameters are not well-constrained. For example, fixing the Hill constant at any value from ~5 to arbitrarily high numbers usually yields fits with similar goodness, while only slightly affecting the determined $EC_{50}$. In other words, the Hill constant estimates reported here represent only a lower limit for the Hill constants. To improve the accuracy of Hill constant estimation, one would need more data points in the transition zone of the dose response curve, at the cost of fewer compounds being tested in parallel on the same plate. However, this is unnecessary for screening applications because the actual value of the Hill constant above the lower limit observed here (Hill > 5) has only a slight effect on the signal in close proximity of the $EC_{50}$.

It may also be necessary to fix the $NCR_{max}$ to get reasonable fits. Such situations are shown in **Figure 5D** and **5F**, where the cytotoxicity of jasplakinolide and swinholide A, respectively, resulted in signal deterioration and limited the useful data available for fitting. (Note that signal deterioration is obvious where the cytotoxicity is higher than the above defined 0.015 threshold). Therefore, the $NCR_{max}$ was made equal to the average NCR of the positive control and kept fixed during the fitting process. This strategy assumes that the cell division proceeds at similar rates in all these experiments. The similar NCR ratios observed for blebbistatin derivatives and cytochalasin D indicate this is a valid assumption, but may not be the case universally. Even if there is a possibility that cell division rates differ, the dense sampling of the dose response curves makes it very unlikely such a difference would introduce more than two-fold uncertainty around the $EC_{50}$ values. All other compounds showed no significant cytotoxicity up to the highest concentration tested (10 µM for blebbistatin derivatives and 500 nM for cytochalasin D). Therefore, the $EC_{50}$ could be easily determined (**Fig. 5A**, **5B**, **5C** and **5E**).

## DISCUSSION

There are several critical steps in the protocol. First, an optimal cell density must be established. Low cell density can result in slow cell growth, unnecessarily long incubation times and total cell numbers that are too low to estimate the signal accurately (see statistical considerations below). Cell density that is too high, on the other hand, will result in extensive overlap of cells. This will interfere with the ability of automated algorithms to correctly identify individual cells and will typically produce an apparent increase of the NCR, as multiple cells are recognized as one cell while individual nuclei are better resolved. Therefore, optimal cell density must be determined in separate experiments for every particular cell line used. For COS-7 cells, we tested a range of 1–6000 cells and found that a surface density of 2000 cells/well

on 96-well plates produced optimal conditions.

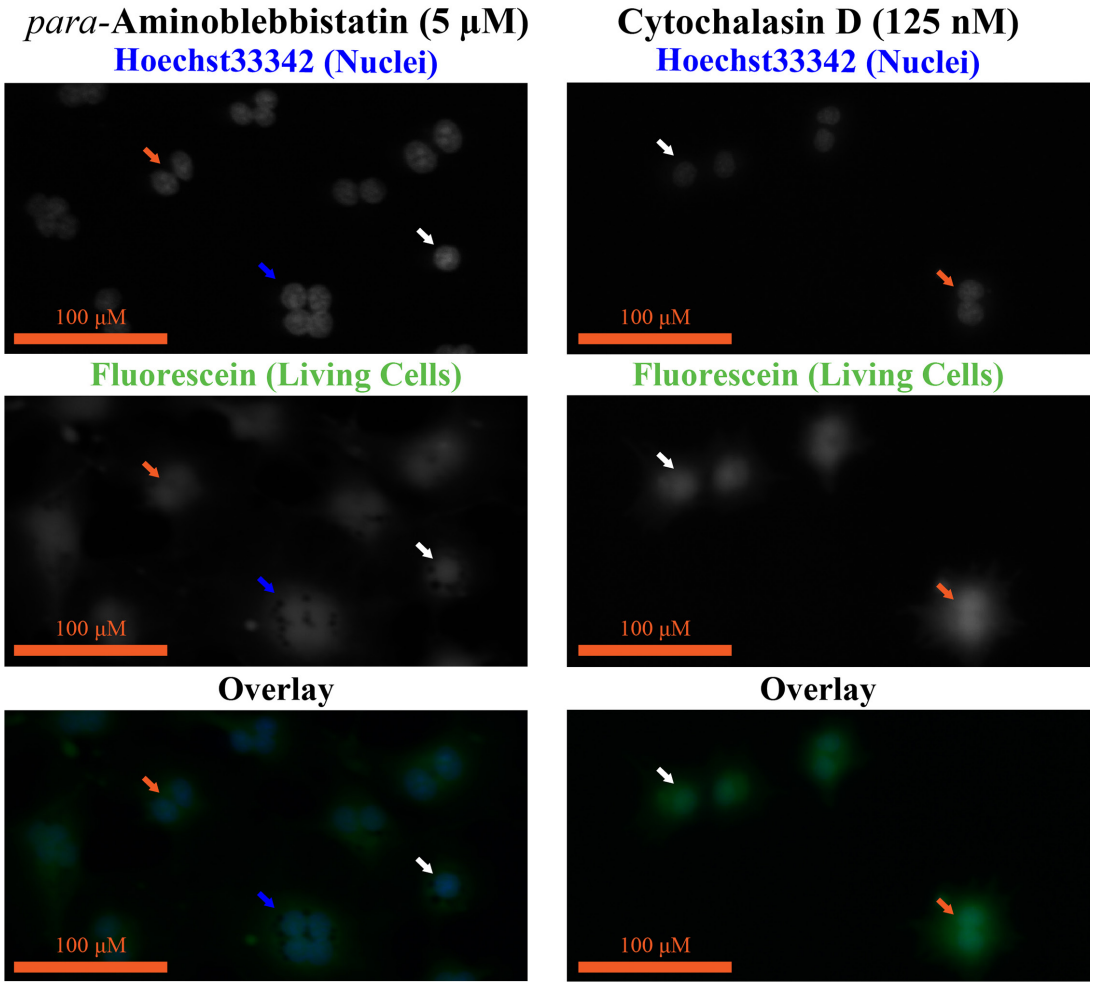


**Figure 4. Cells treated with the NMII inhibitor *para*-aminoblebbistatin (left) or the actin polymerization inhibitor cytochalasin D (right) develop multinucleated phenotype.** Compounds were applied at the concentrations shown in parentheses and the cells were photographed after 24 h of incubation. Images of nuclei (upper panels) and living cells (middle panels) were chosen to include both mono- (white arrows) and binucleated (orange arrows) cells. Occasionally, cells with more than two nuclei were observed (blue arrows). Overlaid images are shown to guide the eyes (lower panels, cytoplasm—green, nuclei—blue). Images were not manipulated other than changing the brightness and contrast for better visibility. No changes were made to the images prior to analysis. PI-positive (dead) nuclei were not observed in these fields of view.

Second, it is highly recommended that compound solutions be diluted in media before adding them to the cell cultures. The density of DMSO is higher than the density of culture medium. Therefore, if DMSO-based solutions are applied directly to cell cultures, DMSO and compound gradients could form within the wells, leading to subsequent compound precipitation, higher cytotoxicity, and/or higher compound concentrations directly above the cell layers. All of these artifacts can be avoided by diluting the compound in media before application. This allows the solutions to be mixed thoroughly by shaking the plate, until a homogenous mixture forms that is relatively dilute for DMSO (2% here, before further 50:50 dilution upon addition to the culture, reaching a final concentration of 1%). This can then be safely applied to cell cultures, as the relatively large, equal volumes (*e.g.*, 100 µl old media + 100 µl compound diluted in media) mix well simply *via* pipetting. The highest tolerated final concentration of DMSO may vary by cell line, but it is typical to go no higher than 1%.

Third, the optimal concentration of FDA, Hoechst33342 and PI, together with the staining time, should be confirmed for each cell line to be used. For instance, because FDA itself is non-fluorescent and the action of esterase enzymes present only in living cells is necessary to hydrolyze it to fluorescein [29,30], staining times that are too short may produce a signal that is not bright enough to clearly identify cells. However, if the incubation time is too long or the FDA solution is not replaced by fresh medium, cells will accumulate too much fluorescein and produce fluorescence that is too bright to easily resolve individual cells. Hoechst33342 and PI parameters can then be modified, if necessary, to fit within the optimal staining time for FDA.

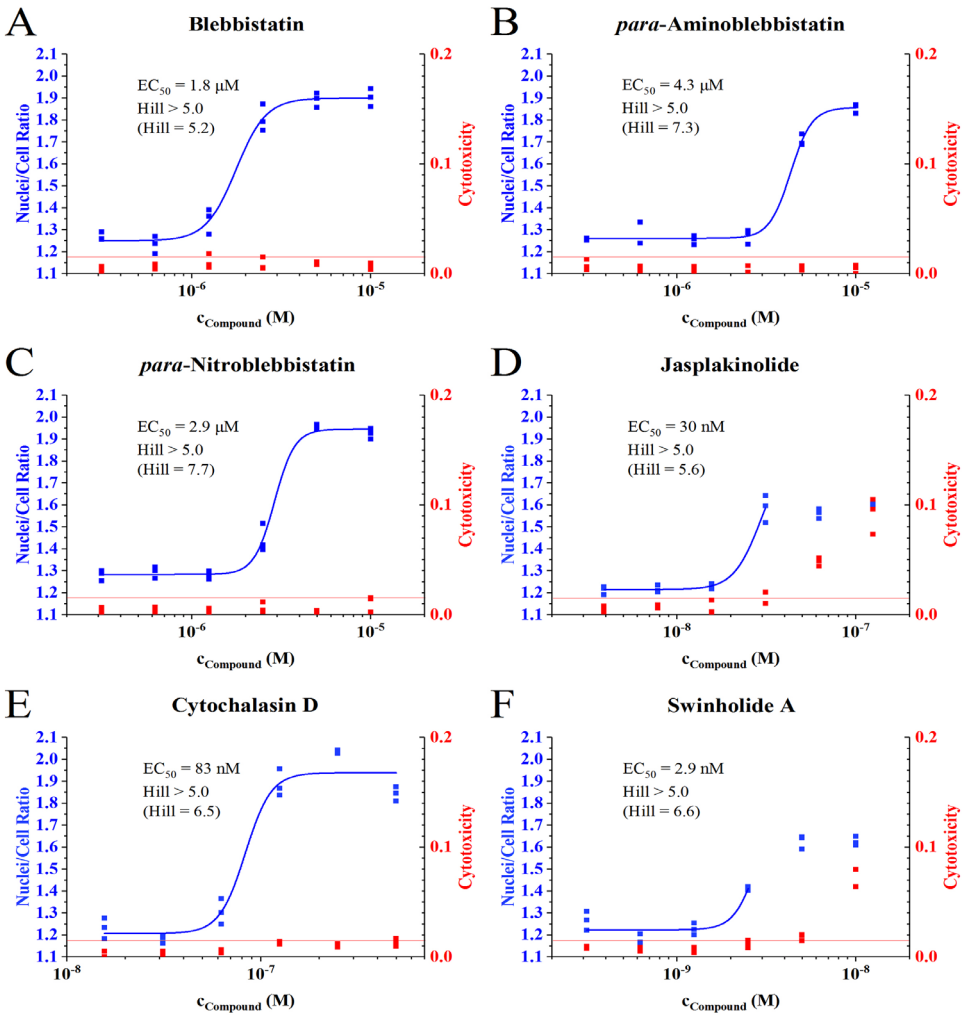


**Figure 5. Determination of compound potency and cytotoxicity.** Representative dose-response curves showing raw data for blebbistatin (**A**), *para*-aminoblebbistatin (**B**), *para*-nitroblebbistatin (**C**), jasplakinolide (**D**), cytochalasin D (**E**) and swinholide A (**F**). Only cells overlapping with nuclei and nuclei overlapping with cells were counted to calculate the primary signal (NCR). Cytotoxicity is calculated as the ratio of dead nuclei to total nuclei. (Here, "total nuclei" is the sum of Hoechst33342 and PI double-positive nuclei and Hoechst33342-positive nuclei overlapping with living cells.) The primary signal was analyzed by fitting the experimental data to the Hill equation. Data points where the associated cytotoxicity signal was above the empirical threshold of 0.015 (red horizontal line, representing a dead nuclei ratio of 1.5%) were disregarded during the fitting process. This threshold usually represents levels of cell death that affect the primary signal (see 10 and 5 nM swinholide A, or 125 and 62.5 nM jasplakinolide as examples). In these cases, it was necessary to assume that the $NCR_{max}$ parameter is equal to the signal of positive control and keep it fixed during the fitting process. In some cases, it might also be necessary to fix the Hill constant to get a reasonable fit. Due to the steep transition of the transition curves, the Hill constant is not well-constrained by the data. Therefore, only a lower limit (~5) can be estimated and reported (the best-fit values are shown in parentheses).

Fourth, the number of cells imaged must be high enough for each well to avoid seriously under- or overestimated signal values, which may occur solely due to the random nature of cell sampling. We have modelled the effect of sample size (number of cells/well) on the accuracy of the estimated signal by assuming that there are mono- and binucleated cells only in the cell population, which is a near-realistic assumption even after 24 h of *para*-aminoblebbistatin treatment (positive control). We further assumed that the ratio of mononucleated cells (in other words the probability of finding a mononucleated cell with random sampling) is $P = 0.85$ and $P = 0.3$ for negative and positive controls, respectively. This yields an expected NCR of 1.15 and 1.7, respectively. (These ratios were determined in preliminary experiments with manual cell counting.) There are exactly $n + 1$ different possible values of the NCR for sample sizes $n > 2$ (except for the extreme situations where all cells are mono- or binucleated). For example, if the sample size was only two cells, there would be only 3 (= 2 + 1) different possible estimated values: 1, 1.5, and 2, for situations where 2, 1 and 0 cells are mononucleated, respectively. Note that this is always true, regardless of the true value of the NCR (*e.g.*, 1.15 and 1.7 above). The probability ($f$) of finding any possible value can be calculated based on the binomial distribution:

**Eqn. 3**, $$f(k,n,p) = \frac{n!}{k!(n-k)!} p^k (1-p)^{(n-k)}$$

where $n$ is the sample size, $k$ is the number of mononucleated cells,

and *p* is the probability of finding a mononucleated cell. Calculating for every possible value yields the probability mass function of the particular distribution. Probability mass functions calculated for several sample sizes are shown in **Fig. 7A**. To improve assay quality (to have a $Z' > 0.5$), it is crucial to obtain "good" estimates of the NCR for every single well. These must be close enough to the true value (*e.g.*, it must fall into the range of true value ± 5%). Because the nature of sampling is probabilistic, the sample size needs to be high enough to achieve this goal. The probabilities of having "good" estimates can be calculated as the sum of the probabilities of all the possible values of the NCR falling into the above defined range (**Fig. 7B**). To ensure that there is less than one well on average for each 96-well plate that might be affected by random sampling issues, this probability must be above 99%, which can be achieved by sample sizes > 300/well. In this work, imaging was continued until at least 600 cells were detected in each well to ensure that final cell numbers are beyond the 300 cells/well threshold. Unfortunately, this threshold of total cell samples represents a limiting factor for further miniaturization of the assay (*e.g.*, 384- or 1536-well plate format).

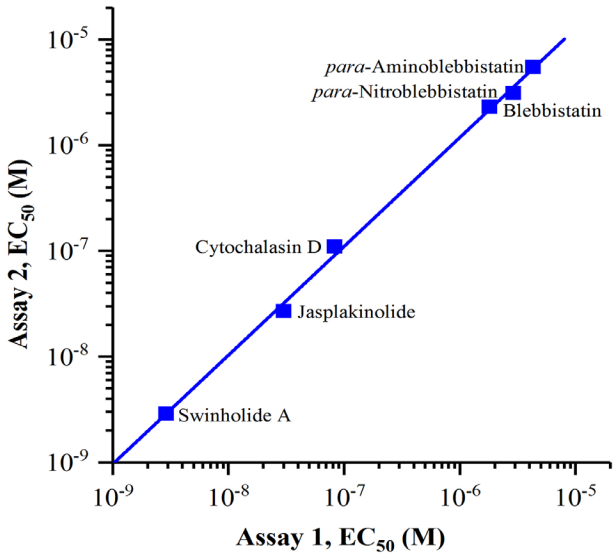


| $EC_{50}$ | | |
|---|---|---|
| **Compound** | **Assay 1** | **Assay 2** |
| Blebbistatin | 1.8 µM | 2.3 µM |
| para-Aminoblebbistatin | 4.3 µM | 5.5 µM |
| para-Nitroblebbistatin | 2.9 µM | 3.1 µM |
| Jasplakinolide | 30 nM | 27 nM |
| Cytochalasin D | 83 nM | 110 nM |
| Swinholide A | 2.9 nM | 2.9 nM |

| Fitting Statistics | |
|---|---|
| Equation | y = a + b*x |
| Intercept | 0.25274 ± 0.14985 |
| Slope | 1.0301 ± 0.02225 |
| Residual Sum of Squares | 0.01627 |
| Pearson's r | 0.99907 |
| R-Square(COD) | 0.99814 |
| Adj. R-Square | 0.99767 |

**Figure 6. Test-retest reliability of the cytokinesis assay.** $EC_{50}$ values (upper right panel) for blebbistatin, *para*-aminoblebbistatin, *para*-nitroblebbistatin, jasplakinolide, cytochalasin D, and swinholide A were determined in two independent runs (assay 1 and assay 2). Compounds showed potencies in a ~1500-fold range. Linear regression analysis (lower right panel) revealed a coefficient of determination ("*R* square") of 0.998 showing that the assay has excellent reliability.

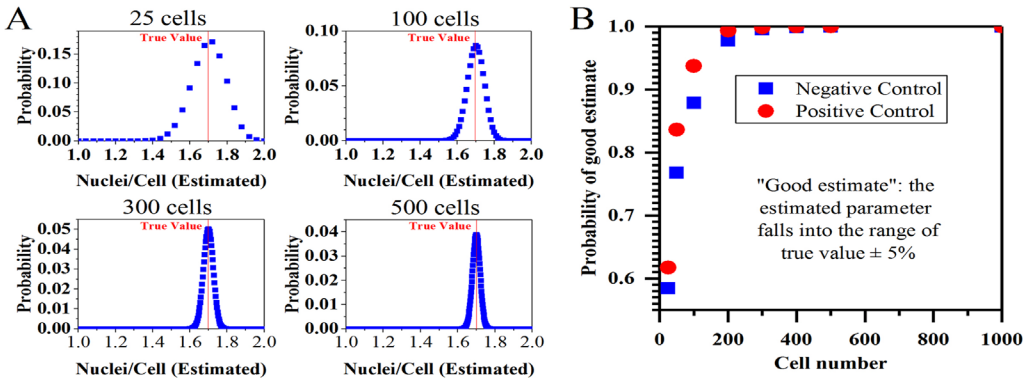


**Figure 7. Assay reliability depends on sample size. A.** Probability mass functions describing the probabilities of finding all possible NCRs depending on the sample size "*n*" (number of cells imaged) were calculated based on the binomial distribution. It was assumed that there are mono- and binucleated cells only and the true value of the NCR is 1.7 and 1.15 for positive and negative controls (not shown), respectively. Note that the probabilities were calculated for discrete values of the estimated NCR, as there are exactly $n + 1$ different possible values of the NCR for sample sizes $n > 2$ (the distributions are not continuous functions). In these calculations, the NCR was always between 1 (all cells are mononucleated) and 2 (all cells are binucleated). True values of the NCR are shown as red vertical lines. **B.** The probability of finding an estimate of the NCR close to the true value can be calculated as the sum of all probabilities falling in the range of true value ± 5% (defined in this work). This probability is highly dependent on the sample size for both positive (red) and negative (blue) controls. Obtaining good estimates is critical to assay reliability (Z-factor). A sample size less than ~300 cells may result in seriously under- or overestimated parameter values solely due to the random nature of sampling.

It is possible that a compound may induce cell loss due to severe cytotoxicity or loss of adherence. In these cases, the above described adaptive imaging strategy (image at least 600 cells) may be limited by the total surface area of a well. If limited cell loss occurs, imaging 600 cells may still be achieved, in which case, this should be further investigated by determining the average number of Hoechst33342-positive nuclei in a unit area imaged for each well in a plate. Nuclei, but not cells can divide in this assay, if an active compound is present. Therefore, if cell loss is negligible, the average number of nuclei (but not cells) in a unit area is expected to always be similar. This ratio should not drop below that of the positive control, unless the compound induces loss of adherence or the conditions in the well(s) are problematic (*e.g.*, contamination).

A similar phenotypic high-throughput screen for the identification of novel cytokinesis inhibitors has been published [10]. In that screen, fixed cells were stained by two dyes to visualize the cytoplasm and nuclei. The requirement for multiple staining and washing steps makes the procedure substantially more time consuming than our current protocol [10]. Moreover, with each step, the risk of losing cells from the surface increases and, because the cells are fixed, cytotoxicity can only be estimated in separate experiments. In contrast, the method detailed here directly applies a single staining step with three dyes to living cells, thereby reducing the risk of cell loss and providing the additional information of a cytotoxicity readout. Others have used EGFP-α-tubulin mCherry-H2B-labeled HeLa Kyoto cells to visualize the multinucleated phenotype after treating cells with blebbistatin derivatives [14,15]. Because these cells express EGFP-α-tubulin in the cytoplasm and mCherry-H2B in nuclei, they do not require any staining before imaging. Although stain-free live cell imaging provides this advantage, one would need to introduce similar genetic modifications to any other cell lines prior to using them in screening experiments. In contrast, the protocol described here uses reagents that are broadly compatible with any cultured cell type. For example, the combination of FDA, PI and Hoechst33342 dyes have recently been used to assess neuronal viability in cerebellar granule neuron cultures [36]. Please see **Table 1** for a summary. Finally, it should be noted that a readout of multinucleation may not be different between inhibition of cytokinesis and induction of cell fusion. To differentiate between the two mechanisms for novel compounds, follow up cell fusion assays could be used [37].

**Table 1. Comparison of the newly developed and previously established cytokinesis assay protocols.**

| | Eggert *et al*. [10] | Kepiro *et al*., Varkuti *et al*. [14,15] | Current protocol |
|---|---|---|---|
| Fixing | Yes | No | No |
| Staining | Yes | No | Yes |
| Dyes used | Tetramethylrhodamine-NHS ester (total cytoplasm)<br>Hoechst33342 (DNA/nuclei) | None | Fluorescein diacetate (living cells)<br>Hoechst33342 (DNA/nuclei)<br>Propidium Iodide (DNA/dead nuclei) |
| Fixing and staining time | ~90 min, 6 steps | No | Staining only, ~15 min, 2 steps |
| Genetic labeling | None | EGFP-α-tubulin (cytoplasm)<br>mCherry-H2B (nuclei) | None |
| Risk of cell loss | High | None | Low |
| Cytotoxicity readout | No | No | Yes |
| Applicability to other cell lines | Yes | Genetic labeling is needed first | Yes |
| Microscopy | Automated fluorescence microscopy | Manual | Automated fluorescence microscopy |
| Image processing | Automated counting of nuclei<br>Manual counting of binucleated cells | Manual | Fully automated (Highly resistant to artifacts) |

In summary, the cytokinesis assay presented here is amenable to semi high-throughput screening applications. It can identify novel cytokinesis inhibitors regardless of their molecular target or mechanism of action, provided that the presence of such inhibitors induce multinucleation. The robustness and flexibility of the assay relies on the simplicity of both the experimental methodology and data analysis. Three inexpensive, small molecule fluorescent dyes are used in combination in a single staining step to provide double-fluorescent labeling for every target of interest, as a readout of compound potency and cytotoxicity. The assay is designed to be resistant to artifacts and has a high rate of reproducibility. Further, the data analysis does not rely on complicated classification of individual cells based on their phenotype. Rather, it simply requires the ability to count cells and nuclei. This can be done by hand or by numerous software programs already programmed to do so automatically.

## Acknowledgments

This work was supported by a grant from the National Institute of Neurological Disorders and Stroke and the National Institute on Drug Abuse NS096833 (CAM, PRG and TMK).

## References

1. McIntosh JR (2016) Mitosis. Cold Spring Harb Perspect Biol 8: doi: 10.1101/cshperspect.a023218. PMID: 27587616
2. Verma V, Mogilner A, Maresca TJ (2019) Classical and Emerging Regulatory Mechanisms of Cytokinesis in Animal Cells. Biology (Basel) 8: doi: 10.3390/biology8030055. PMID: 31357447
3. Leite J, Osorio DS, Sobral AF, Silva AM, Carvalho AX (2019) Network Contractility During Cytokinesis-from Molecular to Global Views. Biomolecules 9: doi: 10.3390/biom9050194. PMID: 31109067
4. Dekraker C, Boucher E, Mandato CA (2018) Regulation and Assembly of

Actomyosin Contractile Rings in Cytokinesis and Cell Repair. Anat Rec (Hoboken) 301: 2051-2066. doi: 10.1002/ar.23962. PMID: 30312008

5. Liu Y, Robinson D (2018) Recent advances in cytokinesis: understanding the molecular underpinnings. F1000Res 7: doi: 10.12688/f1000research.16502.1. PMID: 30542616
6. Atilla-Gokcumen GE, Castoreno AB, Sasse S, Eggert US (2010) Making the cut: the chemical biology of cytokinesis. ACS Chem Biol 5: 79-90. doi: 10.1021/cb900256m. PMID: 20014865
7. Young EJ, Blouin AM, Briggs SB, Sillivan SE, et al. (2015) Nonmuscle myosin IIB as a therapeutic target for the prevention of relapse to methamphetamine use. Mol Psychiatry 21: 615-623. doi: 10.1038/mp.2015.103. PMID: 26239291
8. Young EJ, Briggs SB, Rumbaugh G, Miller CA (2017) Nonmuscle myosin II inhibition disrupts methamphetamine-associated memory in females and adolescents. Neurobiol Learn Mem 139: 109-116. doi: 10.1016/j.nlm.2017.01.001. PMID: 28082169
9. Doller A, Badawi A, Schmid T, Brauss T, Pleli T, et al. (2014) The cytoskeletal inhibitors latrunculin A and blebbistatin exert antitumorigenic properties in human hepatocellular carcinoma cells by interfering with intracellular HuR trafficking. Exp Cell Res 330: 66-80. doi: 10.1016/j.yexcr.2014.09.010. PMID: 25240929
10. Eggert US, Kiger AA, Richter C, Perlman ZE, Perrimon N, et al. (2004) Parallel chemical genetic and genome-wide RNAi screens identify cytokinesis inhibitors and targets. PLoS Biol 2: doi: 10.1371/journal.pbio.0020379. PMID: 15547975
11. Smurnyy Y, Toms AV, Hickson GR, Eck MJ, Eggert US (2010) Binucleine 2, an isoform-specific inhibitor of Drosophila Aurora B kinase, provides insights into the mechanism of cytokinesis. ACS Chem Biol 5: 1015-1020. doi: 10.1021/cb1001685. PMID: 20804174
12. Chieffi P (2018) Aurora B: A new promising therapeutic target in cancer. Intractable Rare Dis Res 7: 141-144. doi: 10.5582/irdr.2018.01018. PMID: 29862159
13. Straight AF, Cheung A, Limouze J, Chen I, Westwood NJ, et al. (2003) Dissecting temporal and spatial control of cytokinesis with a myosin II Inhibitor. Science 299: 1743-1747. doi: 10.1126/science.1081412. PMID: 12637748
14. Képiró M, Várkuti BH, Végner L, Vörös G, Hegyi G, et al. (2014) para-Nitroblebbistatin, the non-cytotoxic and photostable myosin II inhibitor. Angew Chem Int Ed Engl 53: 8211-8215. doi: 10.1002/anie.201403540. PMID: 24954740
15. Várkuti BH, Képiró M, Horváth IÁ, Végner L, Ráti S, et al. (2016) A highly soluble, non-phototoxic, non-fluorescent blebbistatin derivative. Sci Rep 6: 26141. doi: 10.1038/srep26141. PMID: 27241904
16. Bubb MR, Senderowicz AM, Sausville EA, Duncan KL, Korn ED (1994) Jasplakinolide, a cytotoxic natural product, induces actin polymerization and competitively inhibits the binding of phalloidin to F-actin. J Biol Chem 269: 14869-14871. PMID: 8195116
17. Bubb MR, Spector I, Beyer BB, Fosen KM (2000) Effects of jasplakinolide on the kinetics of actin polymerization. An explanation for certain in vivo observations. J Biol Chem 275: 5163-5170. doi: 10.1074/jbc.275.7.5163. PMID: 10671562
18. Brenner SL, Korn ED (1979) Substoichiometric concentrations of cytochalasin D inhibit actin polymerization. Additional evidence for an F-actin treadmill. J Biol Chem 254: 9982-9985. PMID: 489616
19. Carlier MF, Criquet P, Pantaloni D, Korn ED (1986) Interaction of cytochalasin D with actin filaments in the presence of ADP and ATP. J Biol Chem 261: 2041-2050. PMID: 3944126
20. Goddette DW, Frieden C (1985) The binding of cytochalasin D to monomeric actin. Biochem Biophys Res Commun 128: 1087-1092. doi: 10.1016/0006-291x(85)91051-4. PMID: 4004848
21. Goddette DW, Frieden C (1986) Actin polymerization. The mechanism of action of cytochalasin D. J Biol Chem 261: 15974-15980. PMID: 3023337
22. Schliwa M (1982) Action of cytochalasin D on cytoskeletal networks. J Cell Biol 92: 79-91. doi: 10.1083/jcb.92.1.79. PMID: 7199055
23. Mortensen K, Larsson LI (2003) Effects of cytochalasin D on the actin cytoskeleton: association of neoformed actin aggregates with proteins involved in signaling and endocytosis. Cell Mol Life Sci 60: 1007-1012. doi: 10.1007/s00018-003-3022-x. PMID: 12827288
24. Bubb MR, Spector I, Bershadsky AD, Korn ED (1995) Swinholide A is a microfilament disrupting marine toxin that stabilizes actin dimers and severs actin filaments. J Biol Chem 270: 3463-3466. doi: 10.1074/jbc.270.8.3463. PMID: 7876075
25. Bubb MR, Spector I (1998) Use of the F-actin-binding drugs, misakinolide A and swinholide A. Methods Enzymol 298: 26-32. doi: 10.1016/s0076-6879(98)98005-3. PMID: 9751868
26. Zieve GW (1984) Nocodazole and cytochalasin D induce tetraploidy in mammalian cells. Am J Physiol 246: doi: 10.1152/ajpcell.1984.246.1.C154. PMID: 6696055
27. Moulding DA, Blundell MP, Spiller DG, White MRH, Cory GO, et al. (2007) Unregulated actin polymerization by WASp causes defects of mitosis and cytokinesis in X-linked neutropenia. J Exp Med 204: 2213-2224. doi: 10.1084/jem.20062324. PMID: 17724125
28. Kolega J (2004) Phototoxicity and photoinactivation of blebbistatin in UV and visible light. Biochem Biophys Res Commun 320: 1020-1025. doi: 10.1016/j.bbrc.2004.06.045. PMID: 15240150
29. Rotman B, Papermaster BW.(1966) Membrane properties of living mammalian cells as studied by enzymatic hydrolysis of fluorogenic esters. Proceedings of the National Academy of Sciences 55: 134-141. doi: 10.1073/pnas.55.1.134.
30. Guilbault GG, Kramer DN (1966) Lipolysis of fluorescein and eosin esters. Kinetics of hydrolysis. Analytical Biochemistry 14: 28-40. doi: 10.1016/0003-2697(66)90053-4.
31. Arndt-Jovin DJ, Jovin TM (1977) Analysis and sorting of living cells according to deoxyribonucleic acid content. J Histochem Cytochem 25: 585-589. doi: 10.1177/25.7.70450. PMID: 70450
32. Hudson B, Upholt WB, Devinny J, Vinograd J (1969) The use of an ethidium analogue in the dye-buoyant density procedure for the isolation of closed circular DNA: the variation of the superhelix density of mitochondrial DNA. Proc Natl Acad Sci U S A 62: 813-820. doi: 10.1073/pnas.62.3.813. PMID: 4308095
33. Krishan A (1975) Rapid flow cytofluorometric analysis of mammalian cell cycle by propidium iodide staining. J Cell Biol 66: 188-193. doi: 10.1083/jcb.66.1.188. PMID: 49354
34. Edwards BS, Ivnitski-Steele I, Young SM, Salas VM, Sklar LA (2007) High-throughput cytotoxicity screening by propidium iodide staining. Curr Protoc Cytom Chapter 9: doi: 10.1002/0471142956.cy0924s41. PMID: 18770858
35. Zhang JH, Chung TD, Oldenburg KR (1999) A simple statistical parameter for use in evaluation and validation of high throughput screening assays. J Biomol Screen 4:67-73. doi: 10.1177/108705719900400206. PMID: 10838414
36. Jiajia L, Shinghung M, Jiacheng Z, Jialing W, Dilin X, et al. (2017) Assessment of Neuronal Viability Using Fluorescein Diacetate-Propidium Iodide Double Staining in Cerebellar Granule Neuron Culture. J Vis Exp : doi: 10.3791/55442. PMID: 28518109
37. Shinn-Thomas JH, Scranton VL, Mohler WA (2008) Quantitative assays for cell fusion. Methods Mol Biol 475: 347-361. doi: 10.1007/978-1-59745-250-2_20. PMID: 18979254

## Supplementary information

**Figure S1**. Assay plate layout used in screening experiments.

**Figure S2**. Cells treated with the NMII inhibitors blebbistatin (left) and *para*-nitroblebbistatin (right) develop multinucleated phenotype.

**Figure S3**. Cells treated with jasplakinolide (left), an inducer of actin polymerization, or swinholide A (right), an actin severing agent, develop a multinucleated phenotype.

Supplementary information of this article can be found online at http://www.jbmethods.org/jbm/rt/suppFiles/335.